

## Au/TiO<sub>2</sub> nanorod-based Schottky-type UV photodetectors

Hakan Karaagac<sup>\*,1</sup>, Levent Erdal Aygun<sup>1,2</sup>, Mehmet Parlak<sup>3</sup>, Mohammad Ghaffari<sup>1,2</sup>, Necmi Biyikli<sup>1</sup>, and Ali Kemal Okyay<sup>\*\*,1,2</sup>

- <sup>1</sup> Institute of Materials Science and Nanotechnology, Bilkent University, Ankara 06800, Turkey
- <sup>2</sup> Department of Electrical and Electronics Engineering, Bilkent University, Ankara 06800, Turkey
- <sup>3</sup> Department of Physics, Middle East Technical University, Ankara 06800, Turkey

Received 10 September 2012, revised 6 October 2012, accepted 8 October 2012 Published online 12 October 2012

Keywords nanorods, photodetectors, responsivity, Schottky diodes, TiO<sub>2</sub>, hydrothermal growth

 $TiO_2$  nanorods (NRs) were synthesized on fluorine-doped tin oxide (FTO) pre-coated glass substrates using hydrothermal growth technique. Scanning electron microscopy studies have revealed the formation of vertically-aligned  $TiO_2$  NRs with length of  $\sim 2~\mu m$  and diameter of 110–128 nm, homogenously distributed over the substrate surface. 130 nm thick Au con-

tacts using thermal evaporation were deposited on the n-type  $TiO_2$  NRs at room temperature for the fabrication of NR-based Schottky-type UV photodetectors. The fabricated Schottky devices functioned as highly sensitive UV photodetectors with a peak responsivity of 134.8 A/W ( $\lambda$  = 350 nm) measured under 3 V reverse bias.

© 2012 WILEY-VCH Verlag GmbH & Co. KGaA, Weinheim

Today, ultraviolet (UV) photodetection is drawing a significant attention due to its importance in many applications including space communication, environmental monitoring, military and civil applications [1, 2]. Silicon is one of the most widely used materials in UV photodetectors due to its low noise and quick response in the UV region [1, 3]. In spite of these benefits, Si-based UV photodetectors exhibit low efficiency and need costly specific filters to block photons having low energies due to the relatively low band gap. The problems associated with Si-based UV photodetectors can be avoided by the fabrication of UV photodetectors based on wide-bandgap semiconductor materials such as SiC, III-nitrides and most of the II–VI compounds [1, 4].

Among the wide-bandgap semiconductors, TiO<sub>2</sub> can be regarded as the strongest candidate for realization of highly sensitive UV photodetectors due to its outstanding chemical, physical and optical properties [5]. Especially, one-dimensional (1D) TiO<sub>2</sub> structures (nanowires and nanorods) offer great advantages for the realization of highly sensitive UV photodetectors. The incorporation of TiO<sub>2</sub> nanorods (NRs) in a conventional UV photodetector device structure is expected to reduce the recombination probability of electron–hole pairs generated under illumination due

to the presence of surface trap states associated with adsorbed O<sub>2</sub> molecules on the surface of TiO<sub>2</sub> NRs. Although there are many studies reporting the synthesis and characterization of 1D structures of TiO<sub>2</sub>, there is very limited effort to fabricate UV photodetectors based on these structures with Schottky-type device configuration, which is expected to provide higher performance over the conventional p–n junction based devices [6].

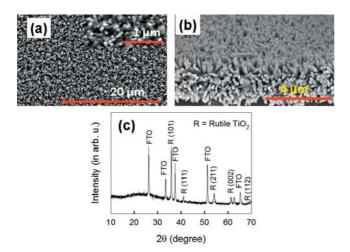
In this investigation,  $TiO_2$  NRs were successfully synthesized by using hydrothermal technique and subsequently employed for the fabrication of highly sensitive UV photodetectors as a device application. The synthesized  $TiO_2$  NRs and the fabricated photodetectors were subsequently characterized in detail by performing several types of characterization measurements.

 $TiO_2$  NRs were grown on pre-cleaned FTO glass substrates by using hydrothermal technique [7]. Following the growth of  $TiO_2$  NRs, to fabricate NR-based Schottky-type UV photodetectors, gold (Au) metallic top contacts were deposited by thermal evaporation using dot (1 mm diameter) patterned 2 × 2 cm<sup>2</sup> copper shadow masks.

Figure 1(a), (b) shows the scanning electron microscopy (SEM) images of TiO<sub>2</sub> NRs grown on FTO glass substrate. It is clear from the images that the diameter and

<sup>\*</sup> Corresponding author: e-mail karaagac@unam.bilkent.edu.tr, Phone: +90 312 290 2513, Fax: +90 312 266 4365

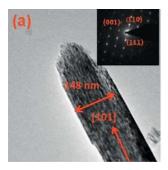
<sup>\*\*</sup> e-mail aokyay@stanfordalumni.org



**Figure 1** (online colour at: www.pss-rapid.com) (a), (b) SEM images of TiO<sub>2</sub> NRs grown on FTO pre-coated glass substrate recorded at different magnifications. (c) XRD pattern obtained for TiO<sub>2</sub> NRs grown on FTO pre-coated glass substrate, showing significant rutile TiO<sub>2</sub> peak with (101) direction.

length of NRs range in between  $110-130\,\mathrm{nm}$  and  $2.0-2.1\,\mu\mathrm{m}$ , respectively. Figure 1(c) presents the X-ray diffraction (XRD) pattern of  $\mathrm{TiO_2}$  grown on FTO glass substrate. As can be seen from the diffraction pattern, all peaks are associated with FTO glass substrate and grown  $\mathrm{TiO_2}$  NRs [8]. The pattern reveals that the peaks are indexed as (101), (111), (211), (002) and (112) corresponding to the rutile structure of  $\mathrm{TiO_2}$ , which is attributed to the growth in strongly acidic solution [8]. From the XRD pattern, it is also observed that R(101) is the most intense peak with respect to the rest of the reflecting planes of the rutile structure, indicating that the  $\mathrm{TiO_2}$  NRs are dominantly oriented in this plane direction.

Detailed structural characterizations of TiO<sub>2</sub> NRs were carried out by performing transmission electron microscopy (TEM) and analyzing associated selected area electron diffraction (SAED) patterns as shown in Fig. 2. The recorded TEM images have revealed that the preferred growth direction is (101) that was obtained from the XRD study as well, indicating the consistency between the re-



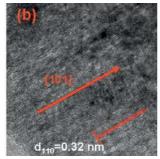


**Figure 2** (online colour at: www.pss-rapid.com) (a) Low-magnification TEM image of TiO<sub>2</sub> NRs and SAED pattern. (b) TEM image recorded with high magnification.

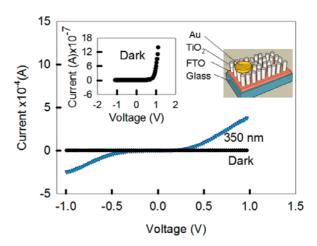


**Figure 3** (online colour at: www.pss-rapid.com) Current–voltage (I-V) characteristics of the fabricated Au/TiO<sub>2</sub>(NRs)/FTO Schott-ky diodes in dark and under light illumination at 350 nm. The inset figures show the dark I-V characteristic and a schematics of the device cross section.

sults of two measurements. From the observed SAED pattern presented in the inset of Fig. 2(a), a set of diffraction spots has appeared and was identified as  $(1\,\bar{1}0)$ , (001) and  $(11\,\bar{1})$  confirming the formation of rutile crystal structure of TiO<sub>2</sub> [7]. In addition, as presented in Fig. 2(b), the space between the adjacent planes was measured to be  $\sim 0.32$  nm, which is in close agreement with the reported (110) lattice constant [7].

Figure 3 shows the current–voltage (I-V) characteristics of the fabricated Au/TiO2(NRs)/FTO Schottky diodes in dark and under light illumination at 350 nm. In addition, the inset figures illustrate the dark I-V characteristics and the schematic cross-section of the fabricated device. It can be seen that the device exhibits rectification under both conditions (dark and light illumination) indicating the formation of a Schottky-type diode with an Au/TiO2(NRs)/FTO sandwich structure. The measured reverse  $(I_R)$  and forward  $(I_F)$  currents at 1 V in dark were found to be around  $1.2 \times 10^{-7}$  A and  $1.4 \times 10^{-6}$  A, respectively and the corresponding rectification ratio is  $I_F/I_R \sim 12$ . The observed significant increase in both reverse and forward currents upon illumination in the UV wavelength range could be attributed to the reduction in the Schottky barrier potential formed between Au and TiO<sub>2</sub>.

Figure 4 exhibits the spectral photoresponsivity of the  $Au/TiO_2(NRs)/FTO$  device measured at reverse biases of 1 V, 2 V and 3 V in the wavelength range of 300–500 nm at room temperature. The responsivity (R) is defined as  $R = I_p/P_{inc}$ , where  $I_p$  is photocurrent and  $P_{inc}$  is the incident illumination power (normal incident on the device), which were measured using white light source (monochromated: 1/8 m grating with 600 lines/mm, and mechanically chopped) together with a lock-in amplifier (SRS830) and a calibrated silicon photodetector, respectively. As seen from Fig. 4, the photoresponsivity is quite low above the wavelength of 410 nm presenting a cut-off wavelength for the



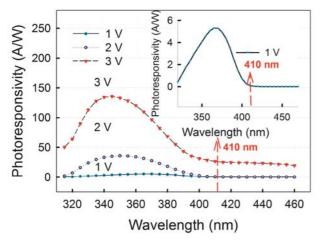


**Figure 4** (online colour at: www.pss-rapid.com) Measured spectral responsivities of the Au/TiO<sub>2</sub>(NRs)/FTO device at different applied reverse biases (1 V, 2 V, and 3 V). The inset shows explicitly the measured responsivity at 1 V reverse bias.

detector. For all measurements conducted at different biases, the photoresponsivity increases with decreasing wavelength, and reaches a peak value at 350 nm and then starts to decrease with further decrease in the wavelength. The enhancement in the responsivity below 410 nm is likely due to the generation of more electron-hole pairs upon illumination of photons with energies larger than that matching the band gap of TiO<sub>2</sub>. Beside this, the decrease in photoresponsivity at lower wavelengths might be attributed to the shorter penetration depth of high energy photons that are absorbed near the surface of TiO<sub>2</sub> NRs as the device is illuminated from the glass side. Therefore, the carrier generation occurs near the TiO2 NRs surface which subsequently triggers the recombination resulting in a decrease in the carrier lifetime [9], since the penetration depth of high energy photons is very short. The measured peak responsivities under illumination of 58  $\mu$ W/cm<sup>2</sup> ( $\lambda = 350$  nm) at reverse biases of 1 V, 2 V and 3 V were 5.3, 36.7 and 134.8 A/W, respectively. As it is expected, the photoresponsivity increases from 5.3 to 134.8 A/W as the bias voltage is increased from 1 to 3 V, indicating the generation of more carriers under Au Schottky contact which allows the effective collection of photo-generated free carriers before recombining or trapping. So far, the reported peak responsivities of fabricated UV photodetectors are in the range of 0.1–13 A/W [6, 10], which are quite lower than that obtained by us with the Au/TiO<sub>2</sub>(NRs)/FTO device configuration. The enhanced UV photoresponsivity observed in this study could be attributed to hole-traps at the

TiO<sub>2</sub> NRs surface incorporated through the adsorbance of O<sub>2</sub> molecules on n-TiO<sub>2</sub> NRs that have a large surface to volume ratio. In other words, adsorbed O<sub>2</sub> molecules capture free electrons from the conduction band of TiO<sub>2</sub> and induce the formation of a highly resistive depletion region near the surface which is responsible for prolonging of the photocarrier lifetime as a result of preventing charge-carrier recombination. Upon UV illumination, the generated holes are trapped by negatively charged O<sub>2</sub> ions that results in unpaired electrons behind, which leads to improvement in charge transportation to the electrodes [9].

In conclusion, high quality TiO<sub>2</sub> NRs were grown on FTO pre-coated glass substrates to fabricate Au/TiO<sub>2</sub>(NRs)/FTO Schottky-type UV photodetectors. Measurements and analysis have shown that the devices give maximum response at 350 nm with a responsivity of 134.8 A/W at 3 V reverse bias. In addition, a significant improvement in responsivity and response time was observed over the Au/TiO<sub>2</sub> thin-film-based Schottky-type UV photodetector, which was attributed to the unique physical and electrical properties of the grown TiO<sub>2</sub> NRs.

**Acknowledgements** This work was supported in part by European Union Framework Program 7, Marie Curie IRG Grants 239444 and 249196 COST NanoTP, TUBITAK Grants 108E163, 109E044, 112M004 and 112E052. The authors acknowledge support from TUBITAK-BIDEB.

## References

- [1] K. W. Liu, M. Sakurai, and M. Aono, Sensors (Basel) 10, 8604 (2010).
- [2] E. Monroy, F. Calle, J. L. Pau, E. Munoz, F. Omnes, B. Beaumont, and P. Gibart, J. Cryst. Growth 230, 537 (2001)
- [3] E. Munoz, E. Monroy, J. L. Pau, F. Calle, F. Omnes, and P. Gibart, J. Phys.: Condens. Matter **13**, 7115 (2001).
- [4] Y. Z. Chiou and J. J. Tang, Jpn. J. Appl. Phys. Part 1 43(7A), 4146 (2004)
- [5] M. Zhang, H. F. Zhang, K. B. Lv, W. Y. Chen, J. R. Zhou, L. Shen, and S. P. Ruan, Opt. Express 20, 5936 (2012).
- [6] J. P. Zou, Q. Zhang, K. Huang, and N. Marzari, J. Phys. Chem. C 114, 10725 (2010).
- [7] M. Ghaffari, M. Burak Cosar, Halil I. Yavuz, M. Ozenbas, and A. K. Okyay, Electrochim. Acta 76, 446 (2012).
- [8] ICSD standard, card number: 169641.
- [9] H. D. Um, S. A. Moiz, K. T. Park, J. Y. Jung, S. W. Jee, C. H. Ahn, D. C. Kim, H. K. Cho, D. W. Kim, and J. H. Lee, Appl. Phys. Lett. 98, 033101 (2011).
- [10] C. Feng, H. Zhang, Y. Wang, W. Li, J. Zhou, L. Chen, L. Yu, and S. Ruan, J. Am. Ceram. Soc. 95, 1980 (2012).